ECCOMAS
Proceedia

BEHAVIOR OF COMPLEX CURVED SURFACE SLIDER IN DESIGN AND EXPERIMENTAL SITUATION

Frederik Bomholt[1], Toshihisa Mano[2]

[1] Technical Group Manager Vibration and Seismic Protection Devices MAURER SE
Frankfurter Ring 193, 80807 Munich
f.bomholt@mauer.eu

[2] Technical Group Manager Testing and Certification MAURER SE
Frankfurter Ring 193, 80807 Munich
t.mano@maurer.eu

Abstract

The performance of curved surface slider (CSS) is in general directly dependent on the dynamic coefficient of friction and the effective radius of curvature. For single CSS and double CSS with non-articulated slider the change of the leading results can be easily determined for the corresponding influence parameter. For more complex CSS, double CSS with articulated slider and adaptive CSS with differences in displacement capacity, coefficient of friction and effective radius of curvature for upper and lower sliding level, the resulting change in performance are much more complex. For the former, differences in coefficient of friction and effective radius can lead to one-sided moving of the slider due to non-geometrical restraint of the inner part. This behavior can lead to significant change in performance with changing restoring stiffness and significant deviations in effective stiffness and damping. Furthermore, the total displacement capacity can be reduced if one-sided sliding occurs with a significant high magnitude.

This change in behaviour is similar for the complex adaptive CSS but much more complex due to the designed sliding behaviour with change from one-sided sliding to simultaneously sliding to one-sided sliding of the other side with each different effective radius and coefficient of friction. The question is how the magnitude of the performance changes due to fluctuating input parameters, here for the coefficient of friction and the effective radius, is a typical task for monte-carlo simulations. In this work the findings of several monte-carlo simulations for a typically double and adaptive CSS will be presented in comparison with experimental results made on appropriate specimens for quality control and type testing.

Keywords: Complex Curved Surface Slider, CSS, Adaptive Isolator, Stochastic Simulation, Experimental Testing,

1   INTRODUCTION

For the mitigation of earthquake loadings, the basic isolation is an established option which can be realized by means of isolator devices [1]. Especially for building of the critical infrastructure like hospitals or main bridges the basic isolation can ensure a high stability and probability of survival of the structure even during big shocks caused by maximum considered earthquakes (MCE). Besides the elastic isolators like high damping rubber bearings or lead rubber bearings the curved surface sliders are well-known products for the application in basic isolation systems. The friction pendulum bearing was developed from the overall movable spherical bearing which commonly will be designed with lubricated sliding material [2]. While a spherical bearing as a part of a bridge bearing system must operate with a minimum of resistance force, the curved surface slider mainly has an additional task of energy dissipation which will be achieved by means of a certain amount of friction. To achieve this friction coefficient the CSS will not be lubricated. The second and more important difference is the additional curvature in the main sliding surface. The evolution of an overall movable spherical bearing with a curvature in the main sliding surface leads to a Sliding Isolation Pendulum bearing with a single sliding surface (SIP-S). Due to the second curvature the CSS achieve a recentering capacity which is dependent on the actual friction of the sliding material as well as the passed horizontal displacement. Because inherently CSS are usable for a stable bearing of high vertical loads, the device does have all characteristics for the requirement of a basic isolation device:

- Vertical load transmission
- Horizontal movement capacity
- Recentering capacity
- Energy dissipation capacity

The last point is optional because a CSS with non-designed energy dissipation can be combined with an energy dissipation device like viscous damper as velocity dependent device or displacement dependent devices like hysteretic dampers.

To improve the second point horizontal movement capacity the SIP-S was further developed to the Sliding Isolation Pendulum bearing with double sliding surfaces (SIP-D). Instead of achieving the pendulum effect by means of a combination of main and secondary sliding surfaces, the SIP-D design has two identical main sliding surfaces which doubles the horizontal movement capacity compared to a SIP-S with almost identical isolator size. As a disadvantage of this improvement of horizontal movement capacity the SIP-D is significantly reduced in rotational capacity because a significant rotation can only occur if one-sided sliding occurs or if the sliding material allow small rotations due to small deformations on the edges. While the former reduces the horizontal movement capacity one-sided and needs in particular high forces to break the frictional resistance of the slider the latter leads to a partial reduction of the sliding gap which is an indicator for the wear of the CSS. This type of isolator is accordingly more related to applications in buildings than in bridges where high demands of rotations and service displacements are requested. But especially for buildings with higher stiffness of the superstructure the SIP-D is the best solution for cost-effective basic isolation systems [3].

A combination of both high horizontal movement capacity and high rotational capacity can be achieved by means of dividing the inner part of the SIP-D into two parts with an additional secondary sliding surface with a sufficient curvature to achieve a SIP-DR, see exemplary Figure 1. This additional hinge allows significant rotation not only in central position but also in a multitude of combinations of horizontal movement and rotational demand. Without any doubt this description fit perfectly to typical mid and width span bridges in seismic regions

which must work properly in service conditions with transmitting forces and translational and rotational movements between the substructure and the superstructure. In the event of earthquakes, the isolation system must provide sufficient decoupling of both parts of the structure by allowing high translational movements in horizontal direction. For this application the use of fully lubricated sliding surfaces is recommended in combination with energy dissipation devices like velocity dependent hydraulic devices. While the latter will have the highest reaction force at around zero displacement because of the highest velocity in this point, the CSS will have the highest reaction force at the maximum out centered position due to the recentering force. This combination leads to a very efficient system with high energy dissipation and low base shear forces acting on the structure. From design point of view the SIP-DR is a double CSS with decoupled sliding surfaces which not automatically slides both simultaneously like a SIP-D but rather only similar sliding occurs if the acting horizontal forces of both main sliding areas are in a certain equilibrium.
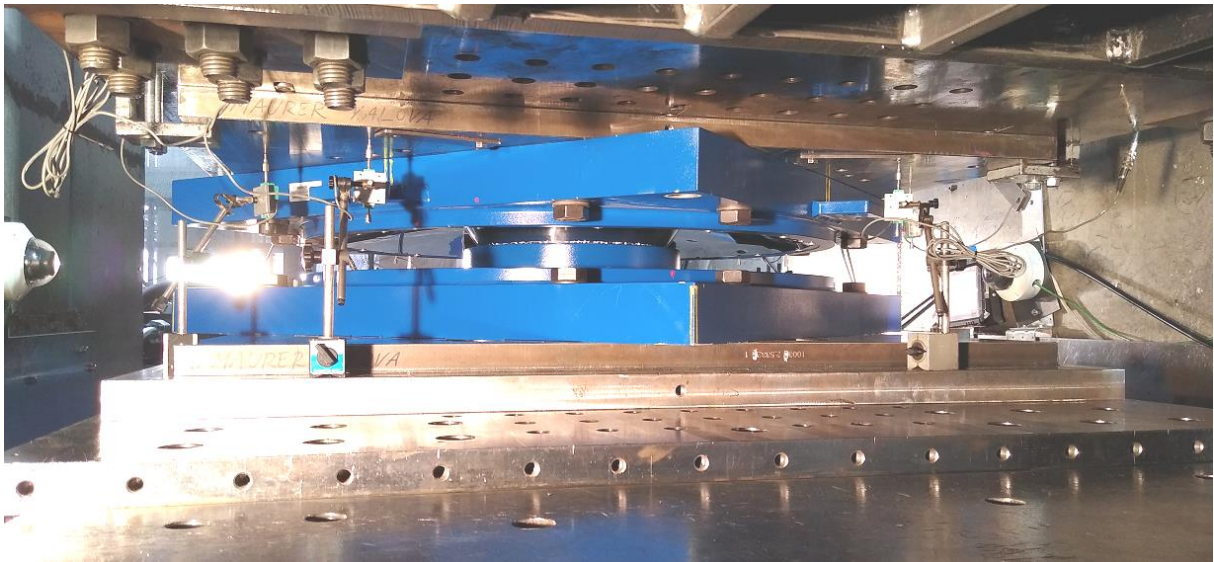

Figure 1: SIP-DR device in test machine of BTS Eucentre, Pavia.

This decoupling of sliding surfaces was the start point for the development of a second generation of CSS with not only decoupled sliding surfaces which shall slide simultaneously but rather which will be controlled for different sliding regimes to achieve different protection levels for different seismic situations. The development results in the adaptive CSS SIP-A [4, 5]. While high frequently earthquakes act with a low magnitude and with low energy impact the isolator must slide with little movements only but with very less friction to reduce the base shear. In case of a design base earthquake the isolator must switch into the second gear to achieve a significant energy dissipation and increase the period of the isolation system. The SIP-A can be designed with an overlapping of siding of both primary sliding surfaces with the different effective radii and design coefficient of friction to have a second working point for the DBE event. Switching into the third gear means for the SIP-A a contact between the bottom part of the slider and the restraint system of the lower sliding plate to allow sliding on the top surface only with the highest displacement capacity and with sufficient amount of design friction and restoring stiffness which are designed to meet the challenges of a maximum considered earthquake (MCE) [6]. The schematically development of the sliding isolation pendulum with and without recentering capacity can be seen in Figure 2.

Figure 2: Summary of different SIP types

Like the SIP-DR the SIP-A must work with decoupled main sliding surfaces which only slides simultaneously if the equilibrium between restoring forces and friction forces is achieved. While the restoring stiffness F_{Re} is dependent only on the actual geometry of the CSS (the actual condition of the several curvatures $R_{geo,act,i}$), the actual friction force F_F is dependent not only on the actual pressure but rather on the actual condition of the surfaces, the sliding velocity v and the temperature T [7].

$$F_{Re} = f(N_S, d, R_{eff}) = N \cdot d/R_{eff} \text{ with Reff} = f\{R_{geo,act,i}\} \tag{1}$$
$$F_F = f(N_S, Area, T, v) \tag{2}$$

Obviously, this dependency of the actual forces leads to differences of both the SIP-DR as well as the SIP-A between the design performance and the actual performance. Especially the friction part is charged with a high uncertainty due to the stochastic nature of the dry friction between two materials. But also, F_{Re} can deviate from the design performance significantly due to geometrical inexactness or softness of the connecting structural members. Both stochastic inevitabilities must be considered for the actual expectation of the device performance and the related assessment of the so-called complex curved surface sliders in experimental situations.

2 STOCHASTIC SIMULATIONS

2.1 Mechanical model

The behaviour of a curved surface slider can be described by means of a mechanical model based on the following assumptions and equations. First the acting horizontal forces are driven by the input parameters of the curved surface slider, which are presented in Table 1.

Lower sliding element	Upper sliding element	Description
$d_{1,cap}$	$d_{2,cap}$	Displacement capacity
$R_{eff,1}$	$R_{eff,2}$	Effective radius
μ_1	μ_2	Coefficient of friction

Table 1: Summary of main design parameters of complex CSS

On a sliding level a horizontal force act which comprise on two parts: friction force and restoring force.

$$F_{H,i} = \mu_i \cdot N_S + \frac{d_i}{R_{eff,1}} \cdot N_S \qquad (3)$$

Where N_S is the acting vertical load on the isolator and d_i is the actual displacement on the corresponding sliding level. Each state of the CSS can be described by means of the six parameters plus the acting vertical load N_s and the following equilibrium equation:

$$\mu_1 \cdot N_S + \frac{d_1}{R_{eff,1}} \cdot N_S = \mu_2 \cdot N_S + \frac{d_2}{R_{eff,2}} \cdot N_S \qquad (4)$$

Due to different effective radii, actual displacement and different coefficient of friction, the sliding regime can become in three different states.

$F_{H,1} < F_{H,2}$ Sliding regime 1; only sliding on lower sliding level
$F_{H,1} > F_{H,2}$ Sliding regime 2; only sliding on upper sliding level
$F_{H,1} = F_{H,2}$ Sliding regime 3; sliding occurs simultaneously on both sliding levels

Due to the different displacement capacity the following restrictions must be considered.

$d_1 = d_{1,cap}$ Sliding regime 2, only sliding on upper sliding level due to capacity restriction
$d_2 = d_{2,cap}$ Sliding regime 1, only sliding on upper sliding level due to capacity restriction
$d_1 + d_2 = d_{1,cap} + d_{2,cap}$ No further sliding can occur

With the model equations and the restrictions, a program code was written in VisualBasic Application to determine hysteresis shape and resulting isolator performance indicator which are summarized in the following. Together with the maximum horizontal force, the effective stiffness is an interesting parameter for the seismic designer for modelling the horizontal stiffness of the base isolated building. The effective stiffness can be calculated by means of the maximum horizontal force at maximum displacement.

$$K_{eff} = \frac{(F_{H,max} - F_{H,min})}{(d_{max} - d_{min})} \qquad (5)$$

In the bilinear model curve, the corresponding displacement of the maximum horizontal force is always the maximum displacement of the cycle while in experimental data the peak of horizontal force will be reached slightly before the maximum displacement. Next significant indicator of performance is the energy dissipation of a cycle EDC which can be calculated by means of the enclosed area of the hysteresis loop and is dependent of the friction component of the CSS.

$$EDC = 4 \cdot \mu \cdot N_S \cdot d \qquad (6)$$

With the energy dissipation and the effective stiffness, the calculation of the effective damping of the isolator is possible.

$$\beta_{eff} = \frac{2}{\pi} \frac{EDC}{K_{eff} \cdot (d_{max} - d_{min})} \qquad (7)$$

Due to the direct or indirect dependency of the indicators from the input parameter coefficient of friction and effective radius of the CSS it is obvious that a change in the input parameter will lead to different magnitude of the indicator.

2.2 Monte Carlo Simulations

According to EC8 and EN 15129 upper and lower bounds for the performance of isolators can be set for the assessment of the isolation system [8, 9]. Though the mechanical description of CSS is comprehensive, a significant deviation of the isolator performance indicator can be observed in isolator tests which is nevertheless a result of fluctuating input parameters of the mechanical model. With neglecting the fact that testing machines in particular have difficulties with maintain a constant vertical load into the isolator while high speed displacement occur, the parameter of the vertical load is assumed as non-fluctuating and the horizontal displacement is the controlling variable. It remains effective radius of curvature and the coefficient of friction. The scattering of the first input parameter is mainly dependent of the quality of production and can be assumed as significantly smaller than the latter influence by the coefficient of friction. In general PTFE or similar PE-materials are common for CSS in combination with austenitic steel which is threaten with fine polish for low roughness of the surface. The tribological behaviour of those materials is strongly dependent of pressure and sliding velocity [10]. Both parameters can be controlled in tests but even with constant pressure and sliding velocity a significant scatter can be still observed for the coefficient of friction. The instable pressure and the inherent changing sliding velocity during a cycle with a sinusoidal wave form intensify the scatter of this decisive influence parameter [11]. Additional to an inherent high scatter of the coefficient of friction at an assumed stable pressure the effect of frictional heating must be considered in the evaluation of understanding and assessment of CSS. Frictional heating occurs during the movement of the CSS due to the heating of the PE material which leads to a significant reduction of the dynamic coefficient of friction. The amount of frictional heating can be in general deterministic described by means of the acting pressure and sliding velocity but still a high stochastic amount must be considered [12].

The result of deviations from the design friction, design effective radius and the friction decrease due to frictional heating can be exemplary seen for a typical SIP-DR in Figure 3. The device with a friction of 5% under a load of 10000 kN has an effective radius of 5000 mm which means each sliding level will rotate with R_{eff} = 2500 mm. Considering really bad and very unlikely deviations of each sliding level with a maximum deviation of 0.8 μ and 0.9 R_{eff} for sliding level 1 and 1.2 μ and 1.1 R_{eff} for sliding level 2, the performance of the device obviously change significant almost in the first cycle. The frictional heating was set to a random decrease in each cycle for the sliding surfaces up to 20% to demonstrate an exaggerated example for a maximum possible alteration of the hysteresis curve.
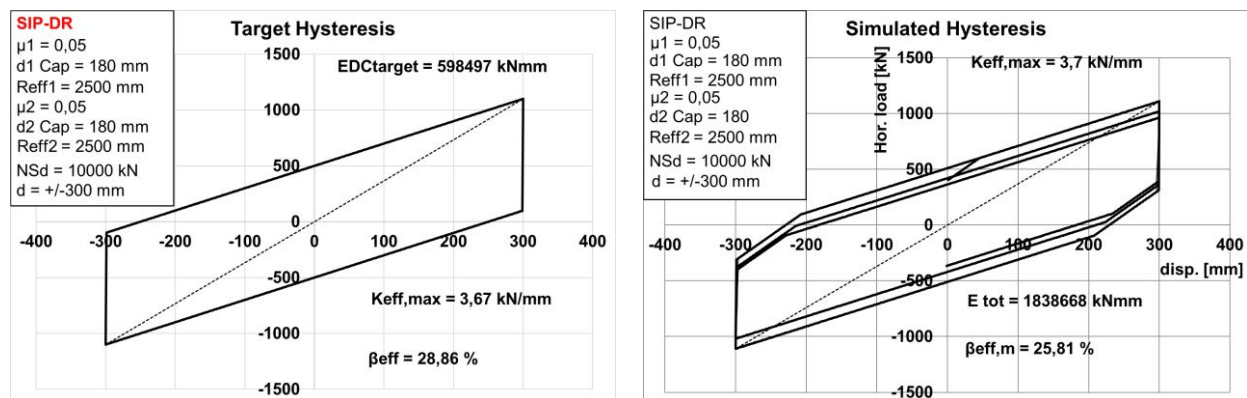

Figure 3: Comparison of target hysteresis and simulated hysteresis for an exemplary SIP-DR device.

For the Monte-Carlo-Simulation all three in detail unknown characteristics – effective radius of curvature, dynamic coefficient of friction and frictional heating – were generated by means of an expectation design value and an upper and lower bound level for each variable. The expression between the bound levels was selected randomly by means of the VBA random function which generates an equal distributed value between the boundaries. The bounds for μ were chosen to 0.8 and 1.2 to reflect the large scatter of friction. For the effective radius of each sliding surface the bounds were set to 0.9 and 1.0. The bounds for frictional heating were always from 0% to 15% for each new cycle i+1 with no frictional heating in the first cycle. For n = 100 simulations as well as for n = 1000 simulations the distribution of results can be seen exemplary for the effective stiffness and the effective damping in Figure 4. A review of stochastic simulations with n = 100 and n = 1000 with the same input parameters show no significant improvement for a number of simulations above n = 100.
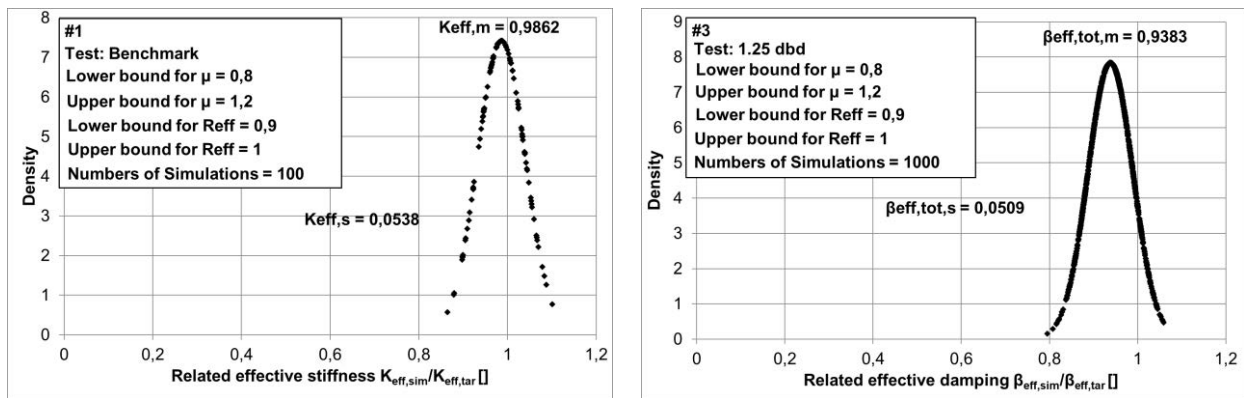
Figure 4: Distribution of related results from simulations with parameters of campaign #1 and #3.

3   EXPERIMENTAL STUDIES

3.1   General description

According to EN 15129 anti-seismic devices must be tested either as initial type tests (ITT) for a first qualification of the device or as part of a factory production control (FPC) with a reduced program compared to the initial type tests [8]. Latter is applicable if the manufacturer already tested similar devices with deviations in terms of friction, maximum load, and geometrical radii with certain tolerance levels. In both tests procedures the execution of a benchmark test is requested for CSS which is a dynamic test executed with the amplitude of +/- d_{bd} and with the vertical design load of N_{Sd}. To allow the execution of the benchmark test in a multitude of test facilities the velocity demand is reduced to only 50 mm/s which is in most cases far below the design velocity of v_{Ed}.

For a statistical comparison the benchmark tests are most valuable because the results of a great number of tests are showing the distribution of performance. In the following the outcomes of two greater campaigns with 26 and 48 specimens tested for quality control will be used in comparison with the corresponding design performance from a statistical point of view. In both campaigns each one type of SIP-DR device was designed, manufactured, and tested. In Figure 5 the related results of β_{eff} can be seen for both the experimental tests and the stochastic simulations.
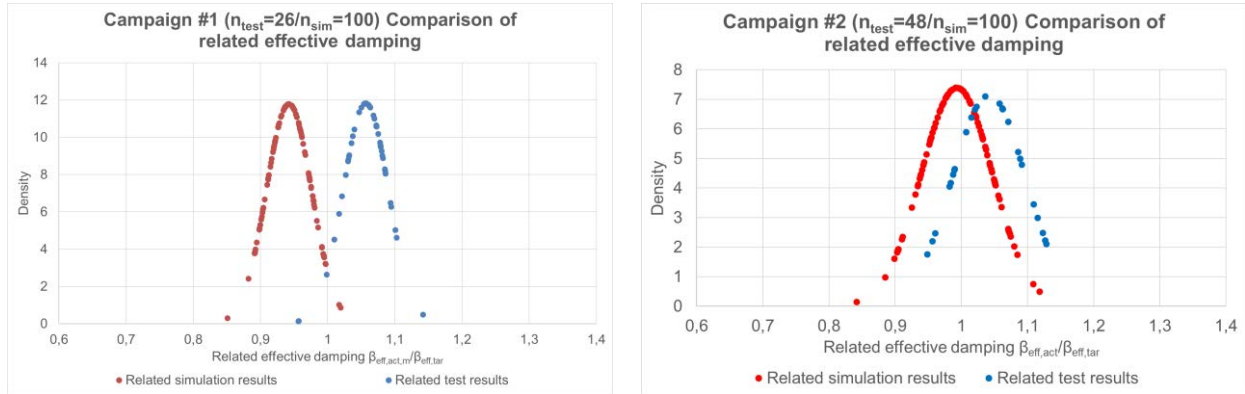
Figure 5: Comparison of distribution of test results and simulation results for the related β_{eff}.

A third test campaign will be finally used which contains the performance of a SIP-A device for which three specimens were tested according to the ITT procedure. Here only less statistical information can be collected but the comparison between theoretical and experimental outcomes will give a precious outlook to the applicability of a stochastically view to the performance of complex CSS.

For all performance results of experimental tests and stochastic simulations the mean of three cycles were used with exception of the maximum horizontal force for which the maximum value is mandatory.

3.2 Findings of the experimental studies

The findings of both experimental result and simulation results are presented in Figure 6 and Figure 7. Both experimental and simulated results are showing the highest scatter in the performance of the mean EDC. With exception of the effective damping all experimental performance indicators are significantly higher than the simulated results which is a result of the velocity effect of dry friction of sliding materials. As described above, the test velocity is significantly less than the design velocity for which the design friction can be controlled. For each of the here described outcomes β_{eff} has the smallest dependency of the increase in friction.
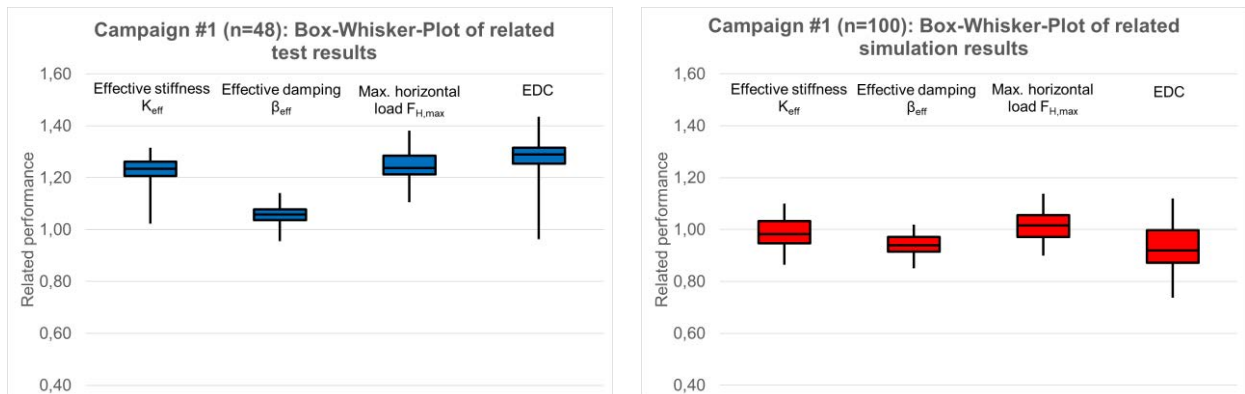

Figure 6: Comparison of SIP-DR performance from tests (left) and simulation (right) from campaign #1.
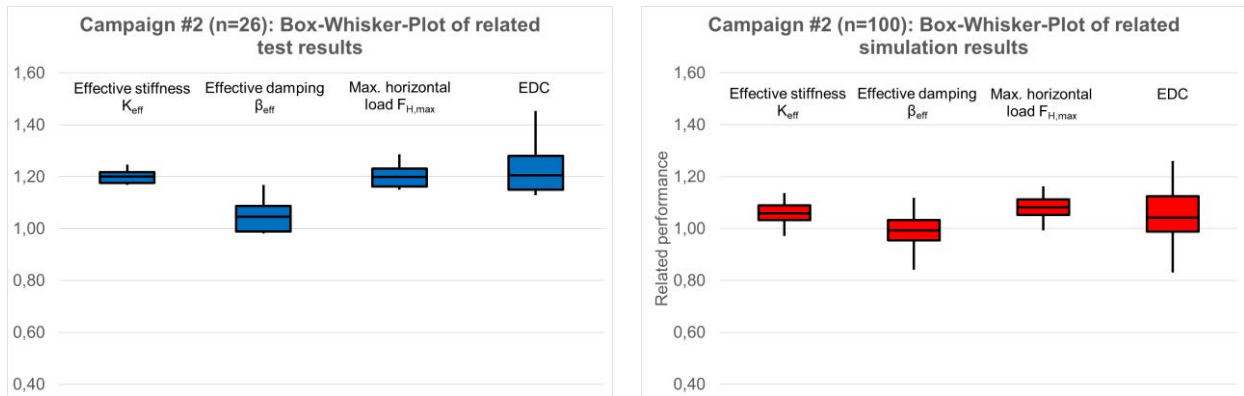
Figure 7: Comparison of SIP-DR performance from tests (left) and simulation (right) from campaign #2

In the next Figure 8 the stochastic simulations will be compared with the performance of the type tests on three SIP-A devices. The comparison was made for an extra dynamic test with 1.25 of d_{bd} which was executed to proof the elevated performance of adaptive CSS beyond the DBE. From the distribution of the test results, a good repeatability of the performance was achieved for all three prototypes. In comparison with the simulation results it becomes obvious that in the simulation significantly too high values for effective stiffness and maximum load will be produced. Because of the simplified model several effects like the velocity effect of a sinusoidal wave form were not simulated. This effect for example reduces the reaction force in the last few percent of movement where the target hysteresis would have a steady increase. In contrast to that observation the effective damping in the tests were significantly higher than evaluated in the simulations. This directly affects the calculation of K_{eff}.
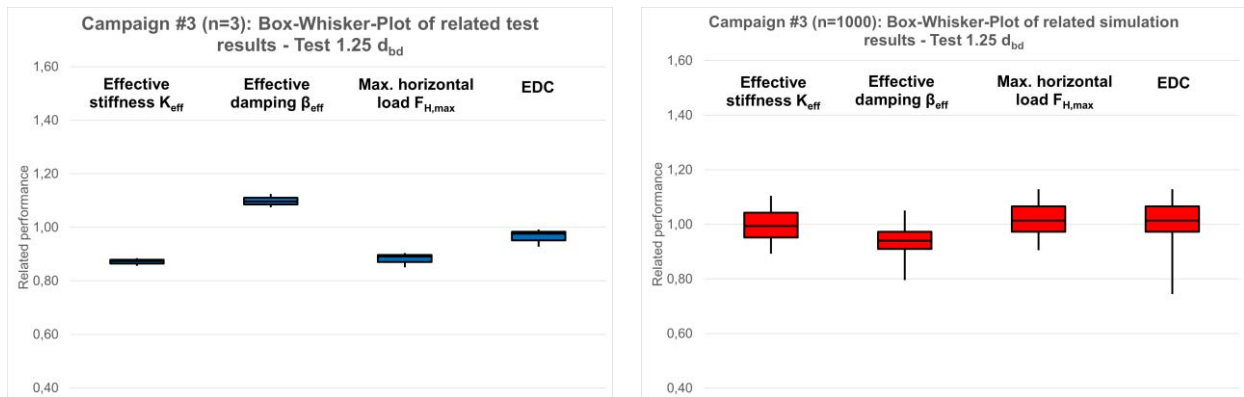

Figure 8: Comparison of SIP-A performance from tests (left) and simulation (right) from campaign #3 for test with 1.25 d_{bd}.

In the next step the development of the deviation from small amplitudes to maximum amplitudes will be checked from a stochastic point of view. By means of the results of the tests D1, D2 and D3 this development can be determined. While test D3 will be carried out with d_{bd}, v_{Ed} and N_{sd}, the tests D1 and D2 will be carried out with only 0.25 d_{bd} and 0.5 d_{bd} but still with v_{Ed} and N_{Sd}. In Figure 9 the development of the related performance is shown for 0.25 d_{bd} to 1.25 d_{bd}. It can be seen that in the test campaign the related values for K_{eff} and the $F_{h,max}$

will decrease with increasing displacement while the related values for β_{eff} increase. In contrast to that the development of the simulation results are less flexible and have steady quantil values while in the tests the magnitude and distribution of the quantil compared to the median fluctuates more intensive, as can be seen in Figure 10. This can be explained by the smaller number of test results compared to the simulation results. Additionally, the mechanical model is not capable to calculate several effects of the test environment which influences the results significantly. Besides the velocity effect mentioned above, in tests with smaller amplitude but with same test velocity the control of the vertical load becomes more instable because of the frequent change of direction and consequently a frequent up and down of the isolator. This leads to high vertical load fluctuations which affects the whole isolator performance in a negative manner.
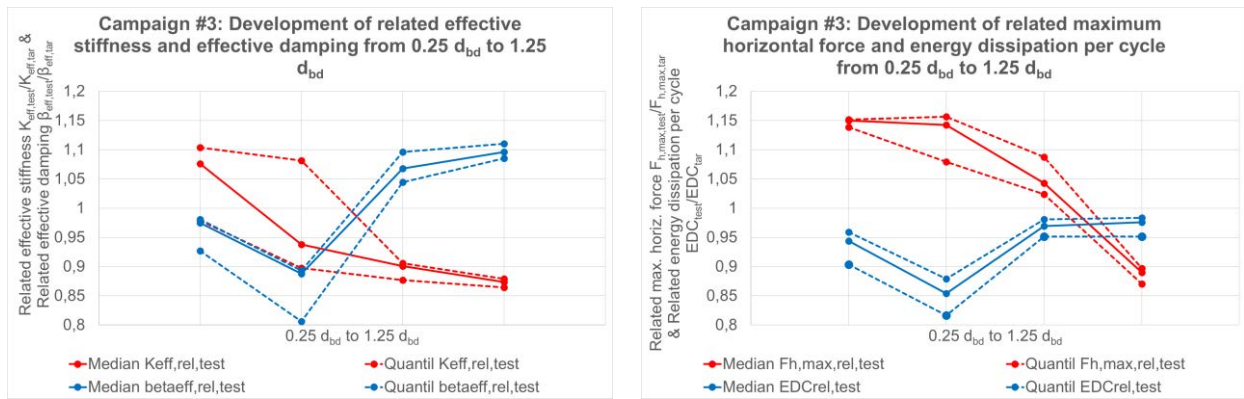

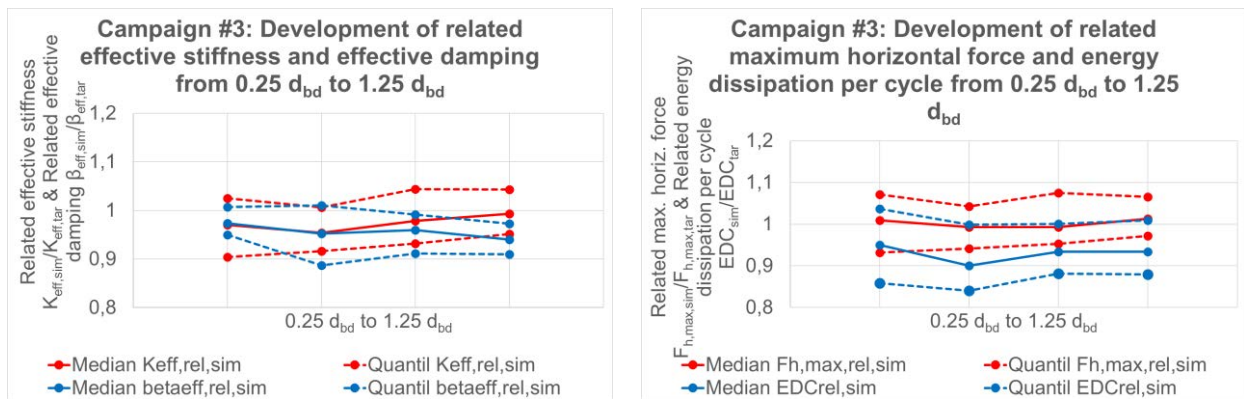Figure 9: Development of SIP-A performance from 0.25 d_{bd} to 1.25 d_{bd} in experimental tests

Figure 10: Development of SIP-A performance from 0.25 d_{bd} to 1.25 d_{bd} in stochastic simulation.

4   CONCLUSIONS

The mechanical background of complex CSS was investigated in this paper with the aim of connecting a mechanical model with a monte-carlo-simulation to achieve a stochastic tool for the assessment of complex CSS like SIP-DR or SIP-A. The model shows a good forecast of isolator performance with considering the stochastic nature of complex CSS which was evaluated by two test campaigns with a significant number of test specimens. For the prediction of single test results the model is fewer applicable because more dynamic effects must be con-

sidered like the velocity effect and the vertical load fluctuations with the corresponding influence on the actual friction.

5   REFERENCES

[1]   C. Casarotti und A. Pavese, „Statistical results of a wide experimental campaign on full scale surface sliders,“ in 2nd European Conference on Earthquake Engineering and Seismology, Istanbul, Turkey, 2014.

[2]   P. Huber und R. Medeot, „The Sliding Isolation Pendulum for the seismic protection of buildings,“ in *WIT Transaction on the Built Environment*, WIT Press, 2008, pp. 323-332.

[3]   F. Weber, T. Mano, H. Distl und C. Braun, „Optimized Triple Friction Pendulum Versus Optimized Double Friction Pendulum,“ in *11th German-Japanese Bridge Symposium*, Osaka, 2016.

[4]   F. Weber, R. Hamood, P. Huber, C. Braun und M. Halimi, „Adaptive Curved Surface Slider for Improved Seismic Structural Performance,“ in *8th International Conference on Seismology & Earthquake Engineering*, Tehran, Iran, 2019.

[5]   F. Weber, F. Obholzer, M. Hartinger und J. Distl, „Adaptive Curved Surface Slider for Improved Seismic Structural Performance,“ *Practial Periodical on Structural Design and Construction,* August 2021.

[6]   F. Weber, L. Meier, J. Distl, F. Obholzer, P. Huber und C. Braun, „SIP-Adaptive: improved structural isolation, reduced base shear,“ in *12th Japanese-German Bridge Symposium*, Munich, Germany, 2018.

[7]   C. Casarotti und A. Pavese, „Statistical results of a wide experimental campaign on full scale surface sliders,“ in *2nd European Conference on Earthquake Engineering and Seismology*, Istanbul, Turkey, 2014.

[8]   Eurocode, *EN 15129: Anti Seismic Devices,* 2009.

[9]   Eurocode, *EN 1998-1: Design of structures for - Part 1: General rules, seismic actions and,* 2004.

[11] C. Braun und C. Butz, „Static and Dynamic Friction in Curved Surface Sliders,“ in *IABSE Symposium: Large Structures and Infrastructures for Environmentally Constrained and Urbanised Areas*, Venedig, Italien, 2010.

[12] S. Barone, A. Pavese und G. Calvi, „Experimental dynamic response of spherical friction-based isolation devices,“ *Journal of Earthquake Engineering,* pp. 2-20, 2017.

[13] D. Domenico, D., G. Ricciardi, S. Infanti und G. Benzoni, „Frictional Heating in Double Curved Surface Sliders and Its Effect on the Hysteretic Behavior: An Experimental Study,“ *Frontiers in Built Environment,* Bd. 5, Nr. 74, 2019.